Reconstruction of SE trade-wind intensity based on sea-surface temperature gradients in the Southeast Atlantic over the last 25 kyr

Jung-Hyun Kim,[1] Ralph R. Schneider,[2] Stefan Mulitza,[1] and Peter J. Müller[1]

Received 18 April 2003; accepted 2 October 2003; published 20 November 2003.

[1] A prominent feature in the Southeast Atlantic is the Angola-Benguela Front (ABF), the convergence between warm tropical and cold subtropical upwelled waters. At present, the sea-surface temperature (SST) gradient across the ABF and its position are influenced by the strength of southeasterly (SE) trade winds. Here, we present a record of changes in the ABF SST gradient over the last 25 kyr. Variations in this SST contrast indicate that periods of strengthened SE trade-wind intensity occurred during the Last Glacial Maximum, the Younger Dryas, and the Mid to Late Holocene, while Heinrich Event 1, the early part of the Bølling-Allerød, and the Early Holocene were periods of weakened SE trade-winds. *INDEX TERMS:* 4267 Oceanography: General: Paleoceanography; 3344 Meteorology and Atmospheric Dynamics: Paleoclimatology; 1620 Global Change: Climate dynamics (3309). **Citation:** Kim, J.-H., R. R. Schneider, S. Mulitza, and P. J. Müller, Reconstruction of SE trade-wind intensity based on sea-surface temperature gradients in the Southeast Atlantic over the last 25 kyr, *Geophys. Res. Lett.*, *30*(22), 2144, doi:10.1029/2003GL017557, 2003.

1. Introduction

[2] An important hydrological feature in the Southeast Atlantic is the Angola-Benguela Front (ABF), the generic convergence between the cold Benguela Coastal Current (BCC) and the warm Angola Current (AC) (Figure 1) [*Shannon et al.*, 1987]. At present, the ABF migrates seasonally between 15° and 17°S off Angola with a typical horizontal SST gradient [*Shannon et al.*, 1987] and delineates the northern boundary of the SE trade-wind field [e.g., *Nelson and Hutchings*, 1983]. North of the ABF, the winds turn clockwise due to the increasing influence of the continental heating on central Africa and induce onshore-directed monsoonal winds [*Peterson and Stramma*, 1991]. Off Namibia, south of the ABF, the SE trade winds induce coastal upwelling during austral winter [e.g., *Nelson and Hutchings*, 1983]. The close linkage between the ABF position and the shift in the direction of the zonal component of the SE trade-wind field along the African coast is related to the extension of the intense coastal upwelling constricted in the north by the ABF [*Lütjeharms and Meeuwis*, 1987]. In addition, SE trade winds influence heat transport from the South Atlantic subtropical zone into the western equatorial Atlantic by affecting the intensity of the South Equatorial Current (SEC) [e.g., *Johns et al.*, 1998]. When SE trade winds are strong, the SEC is subsequently strengthened. At the same time, the South Equatorial Countercurrent is enhanced [*Philander and Pacanowski*, 1986], thus increasing the AC intensity and the heat transport into the region north of the ABF. In conclusion, strong SE trade winds trigger both a cooling south of the ABF due to strengthened upwelling and a warming north of the ABF due to stronger intrusion of warm equatorial waters by the AC. This opposing current regime driven by the trade winds then results in a large SST gradient across the ABF.

[3] For the past 20 kyr, when global climate underwent dramatic changes from an ice age into the Holocene interglacial conditions, there is barely any information regarding the changes in the intensity of Southern Hemisphere atmospheric circulation. Often variations in the amount and composition of lithic grains and pollen in marine sediments are used to reconstruct changes in wind strength [e.g., *Shi et al.*, 2000; *Stuut et al.*, 2002]. However, these "paleo-wind" indicators provide ambiguous information on the changes in wind-intensity, because they may be more dependent on changes in continental climate or in weathering and vegetation cover. In addition, changes in wind trajectories may have altered the lithic grain or pollen signal at a certain site in the marine realm [e.g., *Dupont and Wyputta*, 2003].

[4] In a novel approach, we therefore attempt to reconstruct variations in SE trade-wind intensity over the South Atlantic at centennial to millennial time scales for the last 25 kyr based on temporal variations in Southeast Atlantic SST. For this purpose, following the above described modern situation where the SST gradient across the ABF seems to be strongly related to the intensity of the westerly directed zonal component of the SE trade winds, we selected two marine sediment cores (ODP 1078C and GeoB 1023-5) located north and south of the ABF. Together, these two records provide a high resolution record of variations in SST gradient across the ABF and thus we assume a measure for changes in SE trade-wind intensity over the last 25 kyr.

2. Materials and Methods

[5] ODP 1078C (11°55.24′S, 13°24.01′E) was recovered near the Bight of Angola at a water depth of 426 m [*Shipboard Scientific Party*, 1998] (Figure 1). The age model for ODP 1078C was established by eight accelerator mass spectrometry (AMS) ^{14}C determinations on planktonic foraminiferal tests and mollusks fragments (Table 1). SST estimates were based on the alkenone method [e.g., *Müller et al.*, 1998]. The alkenone-derived SST record from ODP 1078C was compared with that from GeoB 1023-5 (17°09.5′S, 11°00.5′E, 1978 m water depth) [*Kim et al.*, 2002; *Kim and Schneider*, 2003] (Figure 1). Alkenone-derived SSTs can be considered to reflect annual mean SSTs in the upper 10 m of the surface ocean [e.g., *Müller et al.*, 1998]. We thus assume that

[1]Fachbereich Geowissenschaften, Universität Bremen, Bremen, Germany.
[2]Département de Géologie et Océanographie, Université de Bordeaux I, France.

0094-8276/03/2003GL017557

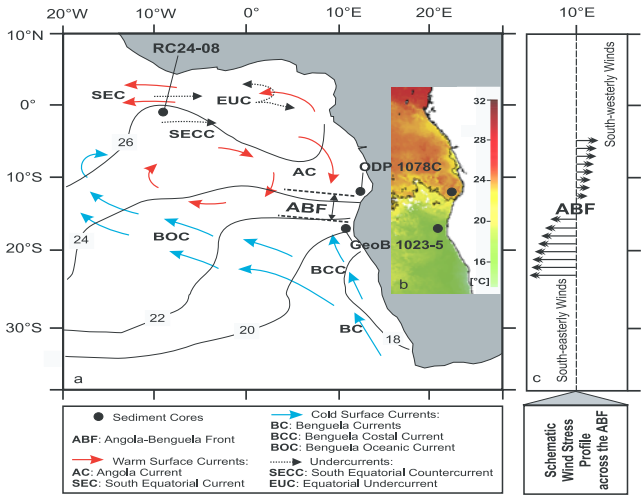

Figure 1. (a) Location map showing positions of sediment cores discussed in this study, the oceanographic setting [e.g., *Shannon et al.*, 1987], and annual mean sea-surface temperatures [*Levitus and Boyer*, 1994] in the Southeast Atlantic. (b) SST distribution pattern in July, 1996 based on Advanced Very High Resolution Radiometer (AVHRR) data from http://podaac.jpl.nasa.gov:2031/DATASET_DOCS/avhrr_pathfinder_sst.html. The black line indicates the 22°C contour. c) Schematic profile of change in the direction of the zonal component of winds across the ABF at 10°E. A meridional component of winds is not represented by the arrows.

differences between two alkenone-derived SST records presented here reflect the annual mean temperature contrast of surface waters across the ABF.

3. Results and Discussion

[6] Figure 2a shows variations in alkenone-derived SST for ODP 1078C over the past 25 kyr north of the ABF. SSTs varied between 22 and 23°C during the Last Glacial Maximum (LGM, 21 ± 2 cal kyr BP) and reached the lowest value of 20.9°C at 16.3 cal kyr BP during Heinrich Event 1 (H1, 18–15 cal kyr BP). Afterwards, the SSTs increased through the course of the deglaciation, indicating a warm period during the time interval of the Younger Dryas (YD, 13–11.5 cal kyr BP). During the Holocene, the SSTs continued to increase to a core-top value of 24.9°C with a slight cooling around 5 cal kyr BP.

[7] Figure 2b shows variations in alkenone-derived SST for GeoB 1023-5 over the past 21 kyr. SSTs in the Southeast Atlantic increased from about 18°C during the LGM to about 21.5°C at 14.5 cal kyr BP south of the ABF. The general warming trend associated with the deglaciation phase continues during H1, but was interrupted by a cold event of about 1000 years duration which corresponds with the YD cold event. Afterwards, the SSTs continued to increase to 22.5°C at about 5 cal kyr BP, and finally decreased to a value of 20.4°C.

[8] The modern annual mean SSTs at the two locations are 25.4 and 19.9°C, respectively [*Levitus and Boyer*, 1994], showing a modern SST contrast value of 5.5°C (Figure 1). In order to evaluate the past variations in SST contrast across the ABF (ΔSST_{ABF}), we subtracted the southern SST record from the northern one (Figure 2c). For the calculation of ΔSST_{ABF}, the data from ODP 1078C and GeoB 1023-5 were interpolated with 100 year time intervals. The obtained ΔSST_{ABF} values range between 1 and 5°C, which we assign to variations in SE trade-wind intensity over the last 25 kyr.

[9] During the LGM and the YD, high ΔSST_{ABF} values suggest an amplified intensity of the SE trade-wind. For H1 and the Early Holocene (EH, 11-8 cal kyr BP), decreasing ΔSST_{ABF} values imply a weakening of the SE trade-wind intensity. During the late part of the Bølling-Allerød (BA, 15–13 cal kyr BP) and the Mid to Late Holocene (MLH, 8–0 cal kyr BP), in contrast to H1 and the EH, the SE trade-wind intensity gradually strengthened. This interpretation is

Table 1. Age control points for ODP 1078C.

Lab no.	Core, Section	Interval [cm]	Depth [cmbsf]	^{14}C age [yr BP]	±Error [yr]	Age[a] [ΔR = 0 yr][b] [cal kyr BP]	Analysed Material
KIA13022	1H-1	30–32	31	1070	35	0.641	planktic/benthic forams & otoliths
KIA13021	1H-1	90–92	91	2490	40	2.132	planktic forams
KIA16170	1H-2	22.5–24.5	174	4210	35	4.294	planktic forams
KIA16169	1H-2	47.5–49.5	199	4900	35	5.259	planktic forams
KIA13018	1H-2	110–112	261	6685	45	7.224	planktic forams/fract. mollusks
KIA13036	1H-3	30–32	331	8570	60	8.996	planktic forams/fract. mollusks
KIA13035	1H-3	60–62	361	8930	70	9.545	snail
KIA13017	1H-4	0–2	451	9520	70	10.281	mollusks
KIA13016	1H-5	0–2	601	10920	90	12.517	planktic forams/fract. mollusks
KIA13025	2H-1	40–42	711	12110	90	13.743	fract. mollusk/scaphopods
KIA13014[c]	2H-1	40–42	711	12260	90	13.815	fract. mollusk/scaphopods
KIA13013	2H-1	110–112	781	12730	80	14.148	fract. mollusk
KIA13026	2H-2	50–52	871	15530	120	17.975	fract. mollusks
KIA13010	2H-2	80–82	901	16990	130	19.655	planktic forams
KIA13009	2H-2	110-112	931	17790	140	20.575	fract. mollusk
KIA13034[c]	2H-2	140-142	961	15780	120	18.262	fract. mollusk
KIA13032[c]	2H-3	0–2	971	16610	+130/−120	19.218	fract. mollusk
KIA13031	2H-3	10–12	981	19070	170	22.048	fract. mollusk

[a]To convert uncorrected ^{14}C ages into calendar ages, the CALIB 4.3 program was used [*Stuiver et al.*, 1998].
[b]Regional ^{14}C reservoir ages (ΔR) are assumed to be 0 year.
[c]not used data for the age model.
The radiocarbon AMS measurements on foraminiferal tests and mollusks were carried out at the Leibniz-Labor, Christian-Albrechts Universität, Kiel, Germany [e.g., *Schleicher et al.*, 1998].

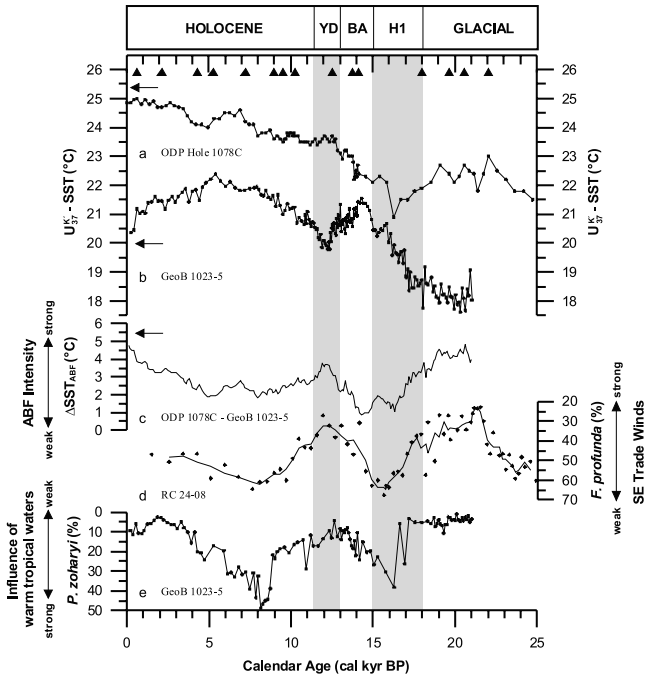

Figure 2. Comparison of SST record from (a) ODP 1078C with that from (b) GeoB 1023-5. The SST record for GeoB 1023-5 is plotted according to the updated age model [*Kim and Schneider*, 2003]. (c) ΔSST_{ABF} is the difference in alkenone-derived SSTs between ODP 1078C and GeoB 1023-5. Data from GeoB 1023-5 were interpolated to match the age model of ODP 1078C. (d) Percentages of the deep-dwelling coccolithophorid *F. profunda* from RC24-08 relative to all other coccoliths [*McIntyre and Molfino*, 1996]. The line represents the three-point running average. (e) Percentages of tropical dinoflagellates *P. zoharyi* from GeoB 1023-5 relative to all other dinoflagellate cysts [*Shi et al.*, 2000]. Solid triangles mark ^{14}C age control points. Vertical grey bars show the H1 and YD time intervals. Arrows indicate modern annual mean SSTs at the location of ODP 1078C (25.4°C) and GeoB 1023-5 (19.9°C) and the corresponding SST difference between the two cores (5.5°C).

consistent with the abundance record of the coccolithophorid *F. profunda* from the equatorial eastern Atlantic (RC 24-08, Figure 2d) which serves as an indicator for nutricline depth and hence SE trade-wind intensity in the equatorial Atlantic [*McIntyre and Molfino*, 1996]. The *F. profunda* record shows that the SE trade-wind intensity was strong or increased during the LGM, the BA, the YD, and the MLH. In contrast, SE trade-wind intensity decreased during H1 and the EH. As a result, the reconstructed SST gradient and the abundance of the coccolithophorid *F. profunda* are very consistent. This result demonstrates that the method used here to reconstruct trade-wind intensities is appropriate and that the three sediment cores considered seem to be coherent. However, more high-resolution SST records from this region are needed to filter out local SST changes which are unrelated to the ABF and thus to verify our results.

[10] Low abundances of dinoflagellates *Polyspaeridium zoharyi* in GeoB 1023-5 during the LGM, the BA, the YD, and the MLH (Figure 2e) [*Shi et al.*, 2000] indicate that warm tropical surface waters did not reach the site of GeoB 1023-5. We can therefore assume that the SST gradient across the ABF was strengthened but the ABF position did not move northward. In contrast, during H1 and the EH, increasing abundances of *P. zoharyi* indicate increasing influence of warm tropical surface waters to the core site of GeoB 1023-5. This implies that, although the ABF position did not migrate southward, the ABF intensity weakens during those periods, resulting in less pronounced SST contrast across the ABF. An evidence for stability of the ABF position over the last 25 kyr relative to the modern position is that both SST records from north and south of the ABF changed in anti-phase (Figures 2a and 2b). This is in agreement with the results of *Jansen et al.* [1996] who showed that during Marine Isotope Stages 1 and 2, the ABF was located close to its modern position between 15° and 17°S.

[11] One likely forcing mechanism that may have controlled changes in the SE trade-wind intensity is low-latitude insolation changes at semi-precessional time scales [e.g., 8.4 and 7.6 kyr, *McIntyre and Molfino*, 1996]. The overall similarity between the ΔSST_{ABF} and *F. profunda* records which indicate SE trade-wind intensity and direct response to wind-driven equatorial divergence, respectively, supports this hypothesis. However, the timing of maxima in SE trade-wind intensity does not exactly fit to periodicities of 8.4 and 7.6 kyr.

[12] Climatic changes initiated in the low-latitudes may have propagated to the high-latitudes [e.g., *McIntyre and Molfino*, 1996], causing variations in the extent of circum-Antarctic sea ice. On the other hand, circum-Antarctic sea ice coverage may have been controlled much more by changes in Southern Hemisphere summer insolation [*Kim et al.*, 1998; *Shemesh et al.*, 2002]. In this context, strengthened SE trade winds during the LGM could be associated with an equatorward expansion of the circum-Antarctic sea ice cover during that period [*Crosta et al.*, 1998], resulting in a northward displacement of the polar front and thus steeper meridional temperature and surface air pressure gradients associated with Hadley Cell circulation [e.g., *Rind*, 1998]. This is supported by grain size and pollen studies in the Southeast Atlantic showing increased humidity in Southwest Africa due to a northward displacement of Westerlies and enhanced SE trade winds during the LGM [*Shi et al.*, 2000; *Stuut et al.*, 2002].

[13] During H1, the weakening of the SE trade-wind intensity was probably related to a pole-ward migration of the polar front in the Southern Hemisphere due to decreasing sea ice [*Shemesh et al.*, 2002] and climate anti-phase behaviour between hemispheres [*Blunier et al.*, 1998]. A renewed northward expansion of the circum-Antarctic sea ice during the BA and the YD [*Shemesh et al.*, 2002] may have re-intensified the SE trade winds. The increase in SE trade-wind intensity during the YD was furthermore associated with global cooling during this period [*Rutter et al.*, 2000]. This study implies that the hypothesis of *Kim and Schneider* [2003] is more likely for the YD than the assumption of thermohaline circulation influence for warming in the tropical western Atlantic [*Rühlemann et al.*, 1999]. The recent study [*Lea et al.*, 2003] shows cooling for the Cariaco basin which is also an argument against overall thermohaline circulation driven warming in the tropical western Atlantic warm pool.

[14] The maximum wet conditions prevailed in Africa during the EH, suggesting that the increase in boreal summer insolation during this period promoted a much stronger monsoonal circulation [e.g., *COHMAP members*, 1988; *DeMenocal et al.*, 2000]. This could have caused a decrease of SE trade-wind intensity as it appears from the reduced SST gradient across the ABF. In contrast, the ΔSST_{ABF} increased towards its maximum value at the end of the Holocene, which coevals with the intensification of Southern Hemisphere summer insolation [*Berger and Loutre*, 1991]. The circum-Antarctic sea ice was absent during the EH and re-advanced during the MLH [*Hodell et al.*, 2001] which, alternatively or in combination with the weakening of the monsoonal system [e.g., *DeMenocal et al.*, 2000], may have caused an increase of SE trade-wind intensity associated with the global cooling observed for the Late Holocene, the so-called Neoglaciation [e.g., *Denton and Karlen*, 1973].

4. Conclusions

[15] In order to investigate past changes in SE trade-wind intensity, we have reconstructed variations of the SST-gradient across the Angola-Benguela Front. The Last Glacial Maximum, the Younger Dryas, and the Mid to Late Holocene were intervals of strong or continuously increasing temperature contrast and inferred strength of SE trade winds. We assume that stronger SE trade winds led to a strong upwelling-related cooling south of the ABF and a warming north of the ABF due to enhanced advection of warm tropical waters by the Angola Current. In contrast, Heinrich Event 1 and the Early Holocene were intervals of decreasing ΔSST_{ABF}. This is attributed to a weakening in SE trade-wind intensity, causing weaker upwelling south of the ABF and less strong warm tropical water transport towards the north of the ABF. The timing of the ΔSST_{ABF} suggests that the expansion or retreat of circum-Antarctic sea ice forced by the southern high-latitude insolation changes seems to be the dominant mechanism for variations in the Southern Hemisphere trade-wind intensity. However, we cannot rule out the possibility that weaker or stronger monsoonal winds caused by the low-latitude semi-precessional insolation cycles changed the strength of the zonal component of trade winds.

[16] **Acknowledgments.** We thank A. Wuelbers and W. Hale at the German ODP Core Repository for providing samples of site 1078C, P. Helmke for his AVHRR-derived SST figure, and two anonymous reviewers for their thorough and constructive comments. Financial support was provided by grants from the German Ministry of Research and Education (BMBF) through the DEKLIM and by the DFG Research Centre Ocean Margins (RCOM contribution No. 0080).

References

Berger, A., and M. F. Loutre, Insolation values for the climate of the last 10 million years, *Quat. Sci. Rev.*, *10*, 297–317, 1991.

Blunier, T., et al., Asynchrony of Antarctic and Greenland climate change during the last glacial period, *Nature*, *394*, 739–743, 1998.

COHMAP members, Climatic changes of the last 18,000 years: Observations and model simulations, *Science*, *241*, 1043–1052, 1988.

Crosta, X., et al., Application of modern analog technique to marine Antarctic diatoms: Reconstruction of maximum sea-ice extent at the last glacial maximum, *Paleoceanography*, *13*, 284–297, 1998.

DeMenocal, P., et al., Coherent high- and low-latitude climate variability during the Holocene warm period, *Science*, *288*, 2198–2202, 2000.

Denton, G. H., and W. Karlen, Holocene climatic variation: Their patterns and possible cause, *Quat. Res.*, *3*, 155–205, 1973.

Dupont, L. M., and U. Wyputta, Reconstructing pathways of aeolian pollen transport to the marine sediments along the coastline of SW Africa, *Quat. Sci. Rev.*, *22*, 157–174, 2003.

Hodell, D. A., et al., Abrupt cooling of Antarctic surface waters and sea ice expansion in the South Atlantic sector of the Southern Ocean at 5000 cal yr B. P., *Quat. Res.*, *56*, 191–198, 2001.

Jansen, J. H. F., et al., Late Quaternary movements of the Angola-Benguela Front, SE Atlantic, and implications for advection in the equatorial ocean, in *The South Atlantic: Present and Past Circulation*, edited by G. Wefer, W. H. Berger, G. Siedler, and D. J. Webb, 553–575, Springer, Berlin, 1996.

Johns, W. E., et al., Annual cycle and variability of the North Brazil Current, *J. Phys. Oceanogr.*, *28*, 103–128, 1998.

Kim, J.-H., and R. R. Schneider, Low-latitude control of interhemispheric sea-surface temperature contrast in the tropical Atlantic over the past 21 kyr: The possible role of SE trade winds, *Clim. Dyn.*, *21*, 337–347, 2003.

Kim, J.-H., et al., Interhemispheric comparison of deglacial sea-surface temperature patterns in Atlantic eastern boundary currents, *Earth Planet. Sci. Lett.*, *194*, 383–393, 2002.

Kim, S. J., et al., Local orbital forcing of Antarctic climate change during the last interglacial, *Science*, *280*, 728–730, 1998.

Lea, D. W., et al., Synchroneity of tropical and high-latitude Atlantic temperatures over the last glacial termination, *Science*, *301*, 1361–1364, 2003.

Levitus, S., and T. Boyer, World Ocean Atlas, vol. 4: Temperature, *NOAA Atlas NESDIS 4*, 117 pp., U. S. Govt. Printing Office, Washington, D. C., 1994.

Lütjeharms, J. E. R., and J. M. Meeuwis, The extent and variability of south-east Atlantic upwelling, in *The Benguela and Comparable Ecosystems*, edited by A. L. L. Payne, J. A. Gulland, and K. H. Brink, 51–62, S. Afr. J. Mar. Sci., 5, 1987.

McIntyre, A., and B. Molfino, Forcing of Atlantic equatorial and subpolar millennial cycles by precession, *Science*, *274*, 1867–1870, 1996.

Müller, P. J., et al., Calibration of the alkenone palaeotemperature index U_{37}^{K} based on core-tops from the eastern South Atlantic and the global ocean [60°N–60°S], *Geochim. Cosmochim. Acta*, *62*, 1757–1772, 1998.

Nelson, G., and L. Hutchings, The Benguela upwelling area, *Prog. Oceanogr.*, *12*, 333–356, 1983.

Peterson, R. G., and L. Stramma, Upper-level circulation in the South Atlantic Ocean, *Prog. Oceanogr.*, *26*, 1–73, 1991.

Philander, S. G. H., and R. C. Pacanowski, A model of the seasonal cycle of the tropical Atlantic Ocean, *J. Geophys. Res.*, *91*, 14,192–14,206, 1986.

Rind, D., Latitudinal temperature gradients and climate change, *J. Geophys. Res.*, *103*, 5943–5971, 1998.

Rühlemann, C., et al., Warming of the tropical Atlantic Ocean and slowdown of thermohaline circulation during the last deglaciation, *Nature*, *402*, 511–514, 1999.

Rutter, N. M., et al., Data-model comparison of the Younger Dryas event, *Canadian J. Earth Sci.*, *37*, 811–830, 2000.

Schleicher, M., et al., The carbonate ^{14}C background and its components at the Leibniz AMS facility, *Radiocarbon*, *40*, 85–93, 1998.

Shannon, L. V., et al., Large- and mesoscale features of the Angola-Benguela Front, in *The Benguela and Comparable Ecosystems*, edited by A. I. L. Payne, J. A. Gulland, and K. H. Brink, 11–34, S. Afr. J. Mar. Sci., 5, 1987.

Shemesh, A., et al., Sequence of events during the last deglaciation in Southern Ocean sediments and Antarctic ice cores, *Paleoceanography*, *17*(4), 1056, doi:10.1029/2000PA000599, 2002.

Shi, N., et al., Correlation between vegetation in southwestern Africa and oceaning upwelling in the past 21,000 years, *Quat. Res.*, *54*, 72–80, 2000.

Shipboard Scientific Party, Site 1078, edited by G. Wefer, W. H. Berger, C. Richter et al., *Proc. Ocean Drill. Program, Init. Repts., 1975*, 143–176, College Station, TX [Ocean Drilling Program], 1998.

Stuiver, M., et al., INTCAL98 radiocarbon age calibration, 24,000–0 cal BP, *Radiocarbon*, *40*, 1041–1083, 1998.

Stuut, J. B. W., et al., A 300 kyr record of aridity and wind strength in southwestern Africa: Inferences from grain-size distributions of sediments on Walvis Ridge, SE Atlantic, *Mar. Geol.*, *180*, 221–233, 2002.

J.-H. Kim, S. Mulitza, and P. J. Müller, Fachbereich Geowissenschaften, Universität Bremen, Klagenfurter Straße, D-28359 Bremen, Germany. (jungkim@allgeo.uni-bremen.de)

R. R. Schneider, Département de Géologie et Océanographie, UMR 5805-EPOC, CNRS/Université de Bordeaux I, Avenue des Facultés, 33405 Talence Cedex, France.